A new CP violating observable for the LHC

Joshua Berger, Monika Blanke, and Yuval Grossman

Institute for High Energy Phenomenology

Newman Laboratory of Elementary Particle Physics

Cornell University, Ithaca, NY 14853, USA

Abstract

We study a new type of CP violating observable that arises in three body decays that are dominated by an intermediate resonance. If two interfering diagrams exist with different orderings of final state particles, the required CP-even phase arises due to the different virtualities of the resonance in each of the two diagrams. This method can be an important tool for accessing new CP phases at the LHC and future colliders.

I. INTRODUCTION

The Standard Model (SM) of particle physics contains a single CP violating phase in the Cabibbo-Kobayashi-Maskawa (CKM) matrix [1]. Many different measurements have confirmed that the SM describes observed CP violation to extremely good accuracy [2, 3]. Particularly strong constraints on physics beyond the SM can be obtained from neutral kaon mixing, pushing the scale of generic new CP violation operators to at least $\mathcal{O}(10^5 \, \text{TeV})$ [4]. Strong constraints have also been obtained from the non-observation of electric dipole moments (see [5] for a review). While one might be tempted to conclude that new physics must be CP conserving up to very high energy scales, this is not necessarily the case. In fact, it is sufficient to introduce the new sources of CP violation in such a way that they are hidden from flavor physics observables. A large new physics scale is not the only way to achieve this; other options include, for example, the introduction of flavor symmetries or decoupling the new sources of CP violation from the flavor sector. Consequently it is important to search for new physics CP violation not only indirectly in low energy observables, such as meson decays or electric dipole moments, but also directly in the production and decay of new heavy particles at colliders. Direct searches have the advantage of giving much cleaner access to the new CP violating phases in question.

In order to observe CP violation in heavy particle decays, asymmetries in the decay rates corresponding to CP-conjugate processes can be measured:

$$\mathcal{A}_{\mathrm{CP}} = \frac{\Gamma(M \to f) - \Gamma(\overline{M} \to \overline{f})}{\Gamma(M \to f) + \Gamma(\overline{M} \to \overline{f})}.$$
 (1)

For this asymmetry to be non-vanishing, the amplitude for the decay rate must be composed of at least two interfering amplitudes with different CP-even ("strong") and CP-odd ("weak") phases. (If the momenta, and possibly the helicities, of the final state particles can be determined, then it is possible to avoid the condition of requiring amplitudes with different strong phases by looking at triple product asymmetries. See e. g. Refs. [6–14].)

In the SM, the weak phase always depends on the CKM phase. More generally, it is related to complex phases of the Lagrangian parameters and, therefore, changes sign under CP conjugation. Strong phases are so-named because they often arise from strong-interaction rescattering of the final state. However, several cases are known where a calculable strong phase arises from the propagation of intermediate state particles. For instance when the two amplitudes arise due to mixing of states with the same quantum numbers, as in $B \to \psi K_S$ for example, the strong phase arises simply through the time evolution of the intermediate $B^0 - \bar{B}^0$ system. Another source of strong phases is finite width effects that have been

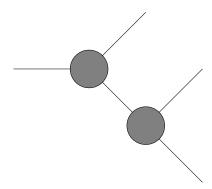


FIG. 1. Diagram demonstrating the presence of a strong phase in the propagator of an intermediate state.

considered in both particle production [15, 16] and decay [17, 18].

The requirement of the existence of a strong phase places a limitation on our ability to measure CP-violation. There is no reason to assume the strong phase is large. Furthermore, there is often no way to determine the strong phase for a given process, since it can involve complicated strongly coupled physics. It is therefore important to look for processes where either the strong phase can be divided out or calculated. Situations where the strong phase can be calculated arise most readily in processes involving a propagating intermediate unstable particle.

In order to see this, consider a diagram of the form shown in Fig. 1. The corresponding amplitude can generally be written in the form

$$\mathcal{M} = \mathcal{M}_1 \frac{1}{q^2 - m^2 + i\Gamma m} \mathcal{M}_2, \tag{2}$$

where $\mathcal{M}_{1,2}$ are, roughly, amplitudes for the upper and lower parts of the diagram and carry the weak phase, q is the off-shell momentum of the propagating particle, m is its mass, and Γ is its width. The Breit-Wigner denominator in this amplitude is CP-even; that is, in the CP-conjugate amplitude, the i in the denominator appears with the same sign. Thus, the propagating particle leads to a strong phase

$$\arg\left(\frac{1}{q^2 - m^2 + i\Gamma m}\right). \tag{3}$$

Recall that in order to have observable CP-violation in a decay process, it is necessary to have at least two amplitudes with different strong phases. If both amplitudes have a propagating particle, then there are two ways in which their strong phases can differ:

1. The propagating particles could be different, so that they have different mass and/or width;

2. The propagating particles could be the same, but off-shell by different amounts.

When studying SM physics, the first situation was considered [17, 18]. In this paper, we study the second case, that is, strong phases that arise from different virtualities. Unlike the SM, this effect is a common feature of heavy particle decays leading to CP violating asymmetries in new physics models. In order to obtain a non-vanishing CP even phase the decay must proceed via two interfering diagrams with the same intermediate unstable particle but with different orderings of the final states. The examples studied in this paper deal with neutral Majorana-like particle decays, i. e. particles that transform under real representations of all symmetry groups. While the appearance of a CP even phase is very natural in such a situation, the mechanism in question is also present in charged particle decays.¹ A concrete example for the latter within the Littlest Higgs model with T-parity will be the subject of a forthcoming publication [19].

The remainder of this paper is structured as follows. In Section II, we discuss general considerations for having a non-vanishing strong phase difference as described above, using a toy model for concreteness. In Section III, we present results of a study of CP violation via that mechanism within a model of new physics, the Minimally Supersymmetric Standard Model (MSSM). We discuss these results and conclude in Section IV.

II. CP-EVEN PHASES IN THE PROPAGATOR

As discussed in the introduction, three conditions must be satisfied in order for a CP-violating asymmetry to be observable in a given process:

- 1. the amplitude must be composed of at least two terms a_1 and a_2 ;
- 2. the two terms must have different CP-even ("strong") phases $\delta_1 \neq \delta_2$;
- 3. the two terms must have different CP-odd ("weak") phases $\phi_1 \neq \phi_2$.

In other words the amplitude must have the structure

$$\mathcal{M} = |a_1|e^{i(\delta_1 + \phi_1)} + |a_2|e^{i(\delta_2 + \phi_2)}. \tag{4}$$

The asymmetry \mathcal{A}_{CP} defined in (1) is then given by

$$\mathcal{A}_{CP} \propto |a_1||a_2|\sin(\delta_1 - \delta_2)\sin(\phi_1 - \phi_2),\tag{5}$$

¹ We would like to thank Alejandro Szynkman for useful discussion that led us to this observation.

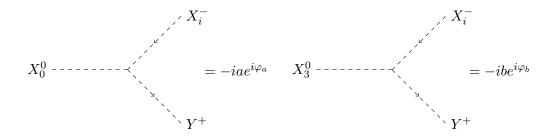


FIG. 2. Feynman rules for the toy model.

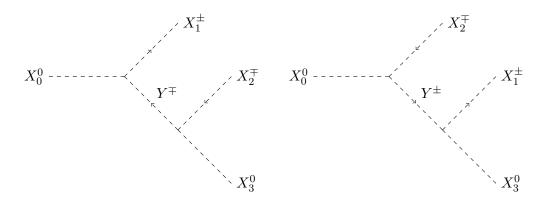


FIG. 3. Diagrams for the decay $X_0^0 \to X_1^{\pm} X_2^{\mp} X_3^0$.

where we see explicitly that the three conditions must be satisfied.

As discussed in the introduction, two decay amplitudes can have different CP-even phases if the intermediate propagating particles are off-shell by different amounts. To make this statement more concrete, consider a three body decay $X_0^0 \to X_1^+ X_2^- X_3^0$. Suppose further that this decay can proceed in two ways

$$X_0^0 \to X_1^+ Y^{-*} \to X_1^+ X_2^- X_3^0, \qquad X_0^0 \to X_2^- Y^{+*} \to X_1^+ X_2^- X_3^0.$$
 (6)

In both cases, the off-shell particle is Y and clearly has the same mass and width. However, its four-momentum in each case is different for a given point in the available phase space of the decay. The two decay modes contribute two different terms to the amplitude which have different strong phases at this point in phase space.

To demonstrate the new CP-even phase, we consider a simple toy model. We assume that all the particles involved are scalars and consider only cubic couplings. We further assume a universality of couplings: the X_0^0 and X_3^0 each couple to the charged particles with the same couplings. While this simplifying assumption is not a necessary condition, it is crucial that all four couplings of $X_{1,2}^{\pm}$ to X_0Y^{\mp} and X_3Y^{\mp} be non-vanishing so that two interfering

diagrams with different final state orderings are present. The Feynman rules we consider are presented in Fig. 2. This toy model has only one physical CP-odd phase,

$$\varphi = \varphi_b - \varphi_a. \tag{7}$$

The diagrams we consider are presented in Fig. 3. The differential decay width can be obtained from the Feynman rules in Fig. 2 and reads

$$\frac{d\Gamma}{dq_{13}^2 dq_{23}^2} = \frac{a^2 b^2}{32(2\pi)^3 m_0^3} \times \frac{1}{(\Delta \hat{q}_{13}^2)^2 + \hat{\Gamma}_Y^2} \times \frac{1}{(\Delta \hat{q}_{23}^2)^2 + \hat{\Gamma}_Y^2} \times \left[\left((\Delta \hat{q}_{13}^2)^2 + (\Delta \hat{q}_{23}^2)^2 + 2\hat{\Gamma}_Y^2 \right) + 2\cos(2\varphi) \left[\Delta \hat{q}_{13}^2 \Delta \hat{q}_{23}^2 + \hat{\Gamma}_Y^2 \right] + 2\sin(2\varphi)\hat{\Gamma}_Y (\Delta \hat{q}_{13}^2 - \Delta \hat{q}_{23}^2) \right] \tag{8}$$

where m_0 is the mass of X_0 , Γ $(\overline{\Gamma})$ is the rate for $X_0^0 \to X_1^+ X_2^- X_3^0$ $(X_0^0 \to X_1^- X_2^+ X_3^0)$ and

$$q_{ij}^2 = (p_i + p_j)^2, \qquad \hat{q}_{ij}^2 = \frac{q_{ij}^2}{m_V^2}, \qquad \hat{\Gamma}_Y = \frac{\Gamma_Y}{m_Y},$$
 (9)

where m_Y and Γ_Y are the mass and width respectively of Y^{\pm} . It is convenient to parametrize the differential decay width using

$$\Delta \hat{q}_{ij}^2 = \hat{q}_{ij}^2 - 1, \tag{10}$$

since we will see that the asymmetry will be largest near the point $q_{13}^2 = q_{23}^2 = m_Y^2$ in phase space.

The first asymmetry that we calculate is the differential rate asymmetry before integrating over phase space:

$$\mathcal{A}_{CP}^{diff} = \frac{d\Gamma/dq_{13}^2 dq_{23}^2 - d\overline{\Gamma}/dq_{13}^2 dq_{23}^2}{d\Gamma/dq_{13}^2 dq_{23}^2 + d\overline{\Gamma}/dq_{13}^2 dq_{23}^2},\tag{11}$$

It is given by

$$\mathcal{A}_{CP}^{diff} = \frac{2\sin(2\varphi)(\Delta\hat{q}_{13}^2 - \Delta\hat{q}_{23}^2)\hat{\Gamma}_Y}{2[1 + \cos(2\varphi)]\hat{\Gamma}_Y^2 + |\Delta\hat{q}_{13}^2 e^{i\varphi} + \Delta\hat{q}_{23}^2 e^{-i\varphi}|^2}.$$
 (12)

Note that this asymmetry is proportional to the sine of the weak phase as desired. Furthermore, it is proportional to $\hat{\Gamma}_Y(\Delta\hat{q}_{13}^2 - \Delta\hat{q}_{23}^2)$. When either $\Gamma_Y = 0$ or $q_{13}^2 = q_{23}^2$ the asymmetry vanishes. This factor in the numerator is proportional to the CP-even phase difference of the two diagrams. We thus demonstrate the occurrence of a CP-even phase due to the virtual Y^{\pm} being off-shell by different amounts in the two diagrams.

The denominator of the asymmetry (12) is minimized when $\Delta \hat{q}_{13}^2 = \Delta \hat{q}_{23}^2 = 0$. That is, when the Y^{\pm} is on-shell in both diagrams. The numerator, however, also vanishes at that point. We thus expect that the points in phase space where the size of the asymmetry is

maximized are near the point $q_{13}^2 = q_{23}^2 = m_Y^2$, along the line $\Delta \hat{q}_{13}^2 + \Delta \hat{q}_{23}^2 = 0$ in order to be as far from the situation where $\Delta \hat{q}_{13}^2 = \Delta \hat{q}_{23}^2$ as possible. In this simple model, we can determine the points of maximum asymmetry analytically and obtain a simple result: the size of the asymmetry is maximized when

$$\Delta \hat{q}_{13}^2 = \pm \hat{\Gamma}_Y \cot(\varphi), \qquad \Delta \hat{q}_{23}^2 = \mp \hat{\Gamma}_Y \cot(\varphi),$$
 (13)

matching our expectation. This result is modified in more complex situations. In particular, when the two interfering diagrams differ in size, the maximum asymmetry is pushed closer to one of the resonances.

Perhaps more telling than the asymmetry itself is the significance of a CP violating signal. The significance of a Dalitz plot asymmetry in a specific bin is given by [23]

$$\sigma_{\rm CP} = \frac{N(i) - \overline{N}(i)}{\sqrt{N(i) + \overline{N}(i)}}.$$
(14)

This quantity depends on the number of X_0 produced, N, so that it cannot be determined without providing further specifications. The relative significance of the bins, however, is of interest as it determines which bins are most important for confirming the existence of an asymmetry. These bins are not necessarily the ones with maximum asymmetry as the differential rate is enhanced near the resonances. There is a tension between the asymmetry which is largest away from the line $q_{13}^2 = q_{23}^2$ and the differential rate which is largest there. In the specific case we are considering, this significance can be written as

$$\frac{d\sigma_{\rm CP}}{\sqrt{dq_{13}^2 q_{23}^2}} = \sqrt{\frac{N}{\Gamma_{X_0}}} \frac{d\Gamma/dq_{13}^2 dq_{23}^2 - d\overline{\Gamma}/dq_{13}^2 dq_{23}^2}{\sqrt{d\Gamma/dq_{13}^2 dq_{23}^2 + d\overline{\Gamma}/dq_{13}^2 dq_{23}^2}},$$
(15)

where Γ_{X_0} is the total width of the X_0^0 .

The Dalitz plots of the differential rate for X_0^0 decay, the rate for the CP conjugate decay, the rate asymmetry, and the significance are given in Fig. 4. To produce that plot we use the following parameters

$$m_0 = 500 \,\text{GeV}, \quad m_1 = 100 \,\text{GeV}, \quad m_2 = 120 \,\text{GeV}, \quad m_3 = 80 \,\text{GeV},$$

 $a = 20 \,\text{GeV}, \quad b = 30 \,\text{GeV}, \quad \varphi = \frac{\pi}{4}, \quad m_Y = 300 \,\text{GeV}, \quad \hat{\Gamma}_Y = 7\%.$ (16)

All of the features discussed above are observed in these plots. The differential rate of X_0^0 decay is largest along two resonances at $q_{13}^2 = m_Y^2$ and $q_{23}^2 = m_Y^2$ with strong interference where the two resonances overlap. Interestingly the interference is constructive above the line

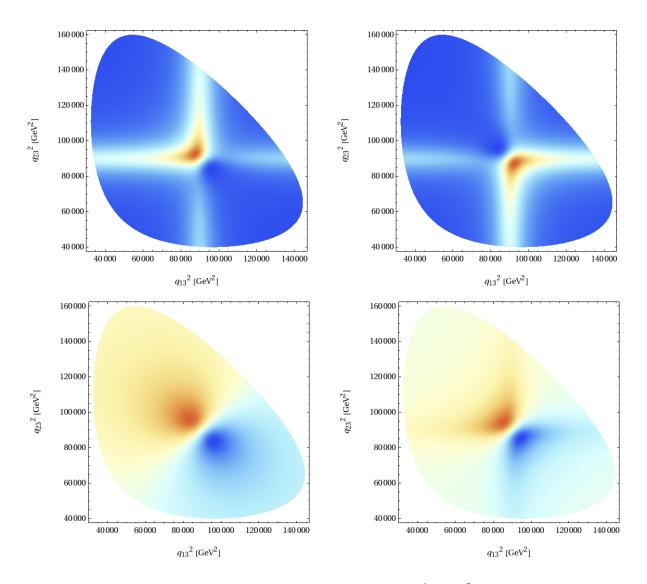


FIG. 4. Dalitz plots for (a) the differential rate of $X_0 \to X_1^+ X_2^- X_3^0$, (b) the differential rate of the CP conjugate decay $X_0 \to X_1^- X_2^+ X_3^0$, (c) the asymmetry \mathcal{A}_{CP} , and (d) the significance $\frac{d\sigma_{\text{CP}}}{\sqrt{dq_{13}^2dq_{23}^2}}\sqrt{\frac{\Gamma_{X_0}}{N}}$.

 $q_{13}^2=q_{23}^2$ while destructive below this line. This feature is reversed for the differential rate of the CP conjugate decay: now the interference is constructive below $q_{13}^2=q_{23}^2$ and destructive above that line, thus exhibiting a clear sign of CP violation. This is made even more explicit in Fig. 4 (c) showing the differential CP asymmetry. The maximum asymmetry is seen to be along the line $q_{13}^2+q_{23}^2=2m_Y^2$, but away from the point $q_{13}^2=q_{23}^2=m_Y^2$. The maximum significance is located closer to the resonances along the lines $q_{13}^2=m_Y^2$ and $q_{23}^2=m_Y^2$.

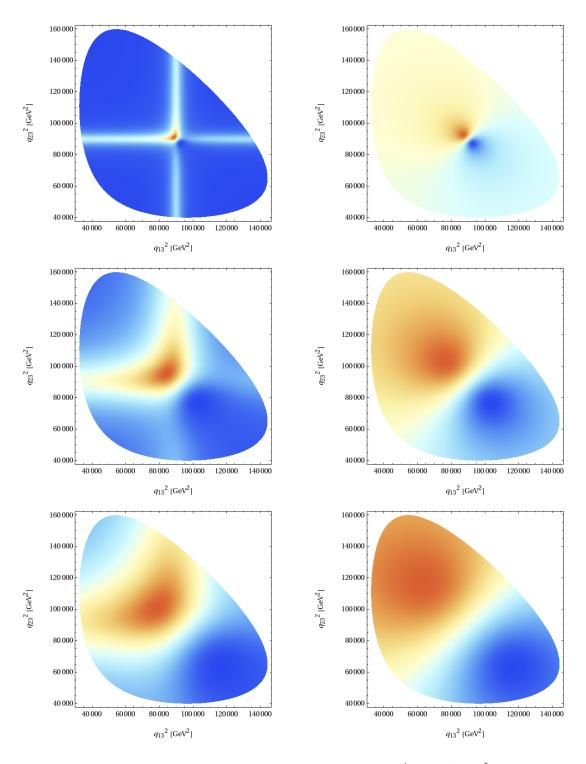


FIG. 5. Differential decay rate and CP asymmetry for $X_0 \to X_1^{\pm} X_2^{\mp} X_3^0$ for $\hat{\Gamma}_Y = 3\%$, 15% and 30% (from top to bottom).

It is instructive to consider how the obtained results change with the width of the intermediate state particle Y^{\pm} . The resonances visible in the Dalitz plot of the differential decay rate should get broader with increasing Γ_Y . Consequently also the differential CP asymmetry is expected to grow and spread further in phase space. These features are clearly visible from Fig. 5 where we show the differential decay rate and CP asymmetry for $X_0 \to X_1^{\pm} X_2^{\mp} X_3^0$ for $\hat{\Gamma}_Y = 3\%$, 15% and 30%, in addition to the corresponding plots for $\hat{\Gamma}_Y = 7\%$ shown in Fig. 4. We therefore expect the effect in question to be particularly pronounced in models which predict strongly coupled resonances.

We now turn to the discussion of integrated asymmetry variables. In general, it is expected that it will be easier to measure the integrated asymmetry. We first discuss the total integrated asymmetry defined as

$$\mathcal{A}_{\rm CP}^{\rm int} = \frac{1}{\Gamma + \bar{\Gamma}} \int dq_{13}^2 dq_{23}^2 \left(\frac{d\Gamma}{dq_{13}^2 dq_{23}^2} - \frac{d\bar{\Gamma}}{dq_{13}^2 dq_{23}^2} \right). \tag{17}$$

Note that the integrated rate asymmetry vanishes in the limit where the particles X_1 and X_2 are degenerate. The asymmetry (12) is anti-symmetric under $q_{13}^2 \leftrightarrow q_{23}^2$, so if phase space is symmetric under such a transformation, the integrated rate asymmetry vanishes. In the case of degenerate charged daughters, phase space has such a symmetry. It is therefore beneficial to weigh the asymmetry above and below $q_{13}^2 = q_{23}^2$ with a relative minus sign and define

$$\mathcal{A}_{\rm CP}^{\rm wgt} = \frac{1}{\Gamma + \bar{\Gamma}} \int dq_{13}^2 dq_{23}^2 \, \operatorname{sgn}(q_{23}^2 - q_{13}^2) \left(\frac{d\Gamma}{dq_{13}^2 dq_{23}^2} - \frac{d\bar{\Gamma}}{dq_{13}^2 dq_{23}^2} \right) \,. \tag{18}$$

Whether or not this asymmetry can be measured is an experimental issue.

Even in this simplified model, we are unable to perform a full phase space integration, due to the rather complex nature of three body phase space. We can, however, integrate over a box around the point $q_{13}^2 = q_{23}^2 = m_Y^2$. The largest contributions to the rate asymmetry will come from within such a box. If the box is a square, then the region of phase space integration is again symmetric and the CP asymmetry vanishes. We could simply use an asymmetric phase space region, but we gain more sensitivity by taking advantage of the sign-weighted asymmetry defined in eq. (18). Integrating over a square box in phase space with width $2wm_Y^2$ centered at $q_{13}^2 = q_{23}^2 = m_Y^2$ and assuming that $\hat{\Gamma}_Y \ll w$, the resulting integrated asymmetry is given by

$$\mathcal{A}_{\mathrm{CP}}^{\mathrm{wgt}} \approx x \log x \sin(2\varphi), \qquad x = \frac{2\Gamma}{wm}$$
 (19)

From the Dalitz plot, we conclude that most of the asymmetry effect is located within such a box. The full asymmetry will then be of the same order of magnitude, with $\hat{\Gamma}_Y \ll w \lesssim 1/4$

required by kinematics. The asymmetry is then proportional to the ratio of the width to some combination of mass scales, with a logarithmic enhancement. The asymmetry is larger for larger width.

In this section, we have worked with the simplest model that exhibits CP-violation where the difference in strong phase between the two diagrams for the process is due to the difference in virtuality of the off-shell particles. The model could be complicated by higher spin particles or by other diagrams. Independent of these complications, we can say a few things about the asymmetries. All of the asymmetries will of course be proportional to the sine of the weak phase difference between the diagrams. The differential rate asymmetry due to the effects described here will always vanish along the line $q_{13}^2 = q_{23}^2$. The integrated rate asymmetry will always vanish if the phase space is symmetric about $q_{13}^2 = q_{23}^2$. By doing a weighted integration over phase space, we can avoid this last constraint and enhance the asymmetry in cases where the two charged particles in the final state are nearly degenerate.

Another possible complication that could arise occurs in the large width limit. We have worked in the Breit-Wigner approximation, which will be valid in the new physics scenario we consider below. If the intermediate resonance is broad, the Breit-Wigner approximation breaks down. This does not alter the qualitative fact that the resonance virtuality leads to a strong phase. We stress that this generic feature of unstable modes in any theory is the crucial one for our purposes.

III. CP VIOLATION IN THE CHARGED HIGGS CHANNEL IN THE MSSM

We now turn to study how this new source of CP violation could be relevant to the MSSM. The electroweak sector of the MSSM is described in Appendix A. That model is a good starting point, since in the limit we are considering it contains only one CP-violating phase, $\text{Im}(\mu^*bM_2^*)$, defined in (A8). Any CP violating observable must involve a process that includes mixing between the Higgs and the electroweak sectors. It turns out that the process

$$\chi_4^0 \to \chi_i^{\pm} \chi_j^{\mp} \chi_1^0, \qquad i \neq j, \tag{20}$$

is very instructive for studying the impact of the strong phases of interest. This process necessarily involves mixing between the Higgs and electroweak sectors. Note that we must be in the limit where the heaviest neutralino is sufficiently heavy that the decay (20) is kinematically allowed. This only occurs when the χ_4^0 is mostly Bino like and the Bino soft mass M_1 is large, that is

$$m_{\chi_4^0} \sim M_1 \gg m_{\chi_i^0}, m_{\chi_i^{\pm}} \sim \sqrt{|\mu M_2|} > m_Z,$$
 (21)

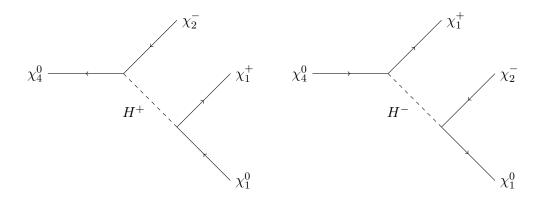


FIG. 6. Decays of a neutralino through a charged Higgs. In this case, there are only two diagrams for the decay.

for i = 1, 2, 3 and j = 1, 2. In order for the decay to be kinematically allowed, the hierarchy must be at least

$$M_1 \gtrsim 3\sqrt{|\mu M_2|}. (22)$$

There are several diagrams for the process $\chi_4^0 \to \chi_i^\pm \chi_j^\mp \chi_1^0$, but we would like to focus on the diagram mediated by the charged Higgs as illustrated in Fig. 6. We further assume that the charged Higgs can decay on-shell in both cases, so that $m_{H^\pm} \gtrsim 2\sqrt{|\mu M_2|}$. In principle, there are also diagrams mediated by the neutral Higgses, the W, and the Z. Diagrams with intermediate W and Z can be neglected since the W and Z are too light to decay on-shell and thus the amplitudes are suppressed compared to the nearly on-shell amplitudes for the Higgses. The lighter neutral Higgs and CP-odd Higgs will also generally be too light to decay on-shell, but the heavy neutral Higgs will generally have a mass $m_{H^0} \sim m_{H^\pm}$. We will, however, neglect all but the diagrams mediated by the charged Higgs for simplicity. If other diagrams were included, then the more familiar type of strong phase would contribute in the interference between these diagrams and the charged Higgs mediated ones.

Before performing some analytic and numerical calculations, we would like to get an idea of how large the CP asymmetry can be in this case. To perform this estimate, we take into account the three sources of suppression that the numerator has relative to the denominator: the weak phase, the strong phase, and, in the integrated case, the required phase space asymmetry. The CP odd effect is proportional to (A8), that is to $|\mu b M_2|$. The relevant dimensionless quantity is normalized to the mass of the decaying particle, that is to some powers of M_1 . Taking $b \sim M_1^2$, which is equivalent to taking $\sin \beta \sim 1$, we conclude that this gives a suppression of

$$\mathcal{A}_{\rm CP}^{\rm diff} \propto \frac{|\mu M_2|}{M_1^2}.$$
 (23)

Numerically, this suppression due to the weak phase is at least about 1/9 due to the kinematic constraint, (22). The requirement of a non-vanishing strong phase implies that the asymmetry is large only in portion of the Dalitz plot with distance of order $m_{H^{\pm}}\Gamma_{H^{\pm}}$ from the point where the two resonances overlap. Thus, for the integrated asymmetry there is an extra suppression of order $\Gamma_{H^{\pm}}/m_{H^{\pm}}$. When considering the fully integrated asymmetry, we get an additional suppression due to the fact that the phase space is nearly symmetric: $\Delta m_{\chi^{\pm}} \ll M_1$. This suppression is not there for the sign weighted asymmetry. This hierarchy gives a suppression of $\Delta m_{\chi^{\pm}}^2/M_1^2$. Putting these pieces together, we can say that for order one CP-odd phase, the asymmetry in integrated rates is roughly given by

$$\mathcal{A}_{\text{CP}}^{\text{int}} \sim \frac{\Gamma_{H^{\pm}} \Delta m_{\chi^{\pm}}^2 |\mu M_2|}{m_{H^{\pm}} M_1^4},\tag{24}$$

and the asymmetry in the weighted rates is roughly given by

$$\mathcal{A}_{\rm CP}^{\rm wgt} \sim \frac{\Gamma_{H^{\pm}} |\mu M_2|}{m_{H^{\pm}} M_1^2}.$$
 (25)

From these results we conclude that, in order to enhance the asymmetry as much as possible, we would like to have the smaller parameters μ and M_2 as close as possible to the larger parameter M_1 without cutting into phase space.

We now present some more specific results. The tree-level differential decay rate induced by the diagrams Fig. 6 is given in Appendix B. In order to study this decay rate, we choose a specific point in MSSM parameter space. We arbitrarily parametrize the model such that the CP-violating phase is contained entirely in μ and the other parameters are real. The Bino mass M_1 is chosen to be much larger than the other weak-scale masses so that there is sufficient phase space to allow the relevant decay. The other new dimensionful parameters are chosen to be of order 100 GeV, but can be varied in absolute scale without changing the results significantly.

The particular choice of parameters used for this study is given in Table I. All other superpartners are assumed to be heavy or otherwise negligible. Dalitz plots of the differential decay rate, relative asymmetry, and significance as defined in Sec. II of the asymmetry for the processes $\chi_4^0 \to \chi_1^{\pm} \chi_2^{\mp} \chi_1^0$, including only the amplitudes involving a virtual charged Higgs, are shown in Fig. 7. Many of the features that were obvious in the toy example are obscured here due to the fact that the resonance in the q_{13}^2 direction corresponding to the left diagram in Fig. 6 is suppressed. In fact using a linear color function for the Dalitz plot (Fig. 7 (a)) this resonance is not even visible and only the dominant one in the q_{23}^2 direction shows up. In Fig. 7 (b) showing the log of the differential decay rate also the q_{13}^2 resonance shows up, but is suppressed by more than two orders of magnitude with respect to the dominant one. The

Parameter	Value	
M_1	$500~{\rm GeV}$	
M_2	$80~{\rm GeV}$	
$\tan \beta$	5	
$M_{H_u}^2$	$-(120 \text{ GeV})^2$	
$M_{H_d}^2$	$(250 \text{ GeV})^2$	
$arg(\mu)$	$\pi/2$	

TABLE I. The choice of MSSM and soft SUSY-breaking parameters used to study CP-violation in the decays $\chi_4^0 \to \chi_1^{\pm} \chi_2^{\mp} \chi_1^0$. All other relevant parameters have been measured and are set to their values according to Ref. [24].

pattern of constructive and destructive interference between the two resonances, which was clearly visible in the toy model decay, is not visible from these figures, suggesting that the relevant CP asymmetry is small. In Fig. 7 (c) we see the resulting differential CP asymmetry which appears "tilted" towards the weak q_{13}^2 resonance with respect to the toy model case. On top of this there is now a phase space dependence in the numerator of the amplitude due to the fact that the external states are not scalars. We also observe the suppression due to the narrowness of the H^{\pm} resonance, $\Gamma_{H^{\pm}}/m_{H^{\pm}} \simeq 0.5\%$.

Next, we calculate CP-violating integrated asymmetries. As discussed in Section II, an unweighted phase space integration can be improved upon by introducing a relative sign between the rates above and below the line $q_{13}^2 = q_{23}^2$ in phase space. In particular, for the scenario described in Table I, the total rate asymmetry is calculated to be -3.5×10^{-5} , while introducing a relative sign improves the asymmetry to -6.5×10^{-4} . The improvement is a factor of almost 20, roughly obtained by eliminating the suppression $\Delta m_{\chi^{\pm}}^2/m_{\chi_4^0}^2 \sim 1/20$.

We have performed this study with the goal of demonstrating the potential relevance of such CP violation to models of physics beyond the Standard Model in general. As such, we have worked from a bottom up approach. In particular, we have worked with a tree-level SUSY Lagrangian with added soft SUSY breaking terms. Renormalization of the parameters from a UV SUSY breaking scheme can significantly alter the spectrum and couplings. Furthermore, a full study of this scenario should include a UV theory of SUSY breaking that gives a heavy, Bino-like neutralino at the weak scale. On the other hand, so long as the phase (A8) is non-zero and the decay studied is allowed to proceed on-shell, the

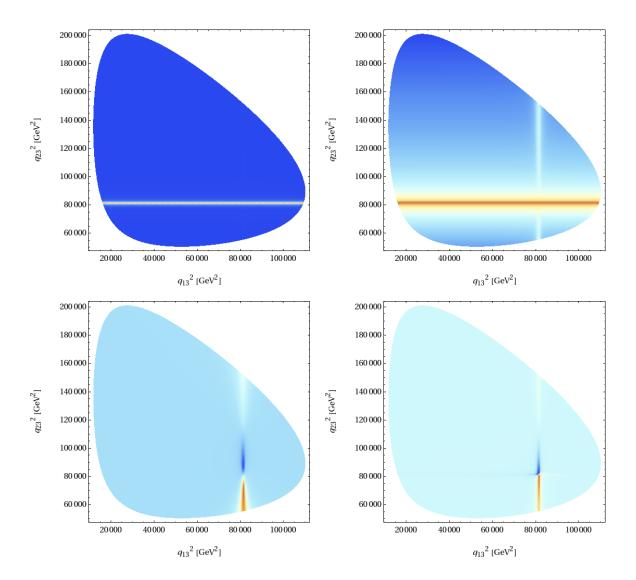


FIG. 7. Dalitz plots for (a) the differential rate of $\chi_1^+\chi_2^-\chi_1^0$ decay, (b) the log of the differential rate, (c) the asymmetry \mathcal{A}_{CP} , and (d) the significance $\frac{d\sigma_{\text{CP}}}{\sqrt{dq_{13}^2dq_{23}^2}}\sqrt{\frac{\Gamma_{\chi_4^0}}{N}}$. The indices 1, 2, 3 refer to χ_1^+,χ_2^- and χ_1^0 respectively.

strong phase due to the virtuality of the intermediate charged Higgs will lead to a new source of CP violation independent of the model's details.

A detailed study of collider prospects of this model is beyond the scope of this paper. We would, however, like to make a few remarks on what would be necessary to observe the asymmetry in question. At the level of theory, a more detailed study should also include the important heavy Higgs contribution. Experimentally, there are several challenges that need to be overcome. Quite generally, the significance of signal depends on the following factors:

the integrated luminosity, the production cross section for χ_4^0 and the branching ratio for $\chi_4^0 \to \chi_1^\pm \chi_2^\mp \chi_1^0$, all affecting the number of events. Due to the smallness of the asymmetry in question clearly a very large number of events is needed. Given a large production of these decays, it is then necessary to identify the events as having the correct structure. In the case where R-parity is conserved, this issue is exacerbated by issues of combinatorics as the heavy neutralino must be produced in conjunction with another superpartner that could have similar decay modes. Our inability to determine final state MSSM particle momenta ensures that we can only determine the integrated asymmetry, which suffers from the additional $\Delta m_{\chi^\pm}^2/m_{\chi_4^0}^2$ suppression. It might be possible to circumvent this suppression by studying asymmetries in kinematic observables, such as invariant masses of the SM decay products of the decaying charginos. We leave such investigations for future work.

IV. CONCLUSIONS

The hope is that new physics will be soon discovered at the LHC. Once it is discovered, we can turn to study all the parameters describing it. In particular, we will study the masses, spins and couplings of the new particles. In doing so, we would like to look for signals of CP violation. In this paper, we pointed out a new way to look for such signals: looking for asymmetries in the Dalitz plots of cascade decays with unstable intermediate particles. The new observation is the fact that a strong phases can arise even when there is only one intermediate particle. This phase is present when there are two amplitudes in which the intermediate particle has different virtuality.

This situation arises generally in cases where two interfering diagrams exist with different orderings of the final state particles. This effect can be present in both neutral and charged particle decays. While we have elaborated mainly on neutral particle decays in this paper, a study of a concrete example of CP asymmetries in charged particle decays is in progress [19]. The new observable we discuss is complementary to other observables that have been discussed before, such as triple product observables and CP violation associated with oscillations.

It is particularly important to account for the kind of strong phase described here in new physics models. Most of these models, and certainly ones in which we can hope to calculate any observables reliably, are weakly coupled at sufficiently low energies. In such cases, a sizable strong phase can only come in processes involving unstable particles. This could be important in essentially any beyond the SM scenario, such as heavy neutrino decays, Kaluza-Klein state decays, and W' or Z' decays, to name just a few examples. Even within

the weak sector of the MSSM, interference terms of the kind studied here are relevant to the asymmetry in $\chi_i^0 \to W^{\pm}H^{\mp}\chi_j^0$, where it is a subdominant contribution compared to chargino mixing. In many of these new physics scenarios, observables could be complicated, as in the MSSM weak sector, by the existence of several amplitudes for the decay, all with different strong phases.

The CP violating observable we have introduced could, in principle, be relevant for SM physics as well, but it is not easy to come up with a practical observable. In terms of fundamental particle decays, a possible channel would in principle be $t \to q_i q_j \bar{q}_k$ with an intermediate W exchange. However, the region where the W is approximately on shell in both diagrams lies outside the physical region of phase space. In addition, the weak phase is highly suppressed due to the hierarchical structure of the CKM matrix strongly favoring one decay channel over the other. We thus have to rely on decays of composite particles, namely hadrons. Indeed, there is a plethora of three body decays of K, D and B mesons at our disposal. Kaon decays, however, do not occur via a resonance. Neutral D and $B_{d,s}$ meson decays are not good examples either, since the same physics can be probed via oscillations in a more effective way. We are thus left with charged B and D meson decays. While it should be possible to find a decay channel for which the intermediate particle can go on shell in both diagrams, we are again confronted with the CKM hierarchy, leading to a strong suppression of one channel with respect to the other in many cases.

To conclude, most extensions of the SM include new particles whose decays can lead to the type of CP violation that we discuss here. Thus, we expect this type of CP violation to be relevant in finding CP violating signals at the LHC and future colliders in many of the possible scenarios for physics beyond the SM.

Acknowledgements

This work is supported by the U.S. National Science Foundation through grant PHY-0757868 and CAREER award PHY-0844667. MB would like to thank Andrzej Buras and the Technische Universität München for the hospitality during the completion of this work.

Appendix A: The Electroweak Sector of the MSSM

The charginos and neutralinos are the mass-basis superpartners of the Higgs and Electroweak gauge bosons. Their physics is determined by three components of the Lagrangian:

• The superpotential

$$W = \mu H_u H_d \tag{A1}$$

leading to fermion terms

$$\mathcal{L} = -\mu \tilde{H}_u \tilde{H}_d + \text{h.c.} \tag{A2}$$

• The supersymmetric gauge interactions

$$\mathcal{L} = -\sqrt{2}g \left(H_d^{\dagger} \frac{\sigma^a}{2} \tilde{H}_d \right) \tilde{W}^a - \sqrt{2}g \tilde{W}^a \left(\tilde{H}_d^{\dagger} \frac{\sigma^a}{2} H_d \right)
- \sqrt{2}g \left(H_u^{\dagger} \frac{\sigma^a}{2} \tilde{H}_u \right) \tilde{W}^a - \sqrt{2}g \tilde{W}^a \left(\tilde{H}_u^{\dagger} \frac{\sigma^a}{2} H_u \right) + \sqrt{2}g' \left(H_d^{\dagger} \frac{1}{2} \tilde{H}_d \right) \tilde{B}
+ \sqrt{2}g' \tilde{B} \left(\tilde{H}_d^{\dagger} \frac{1}{2} H_d \right) - \sqrt{2}g' \left(H_u^{\dagger} \frac{1}{2} \tilde{H}_u \right) \tilde{B} - \sqrt{2}g' \tilde{B} \left(\tilde{H}_u^{\dagger} \frac{1}{2} H_u \right) \quad (A3)$$

• The soft SUSY-breaking interactions

$$\mathcal{L} = -(M_1 \tilde{B} \tilde{B} + M_2 \tilde{W}^a \tilde{W}^a + b H_u H_d + \text{h.c.})$$
(A4)

Notice that the Higgsino mass is determined only by the superpotential, the gaugino mass only by the SUSY-breaking interactions, and the mixing only by EWSB. This structure means that the mass difference between charginos will always be at least of order m_W . This fact will lead to a suppression of CP violating effects in the chargino-neutralino sector, which are generally suppressed when the mass difference is either much smaller or larger than some other scale set by the width in the process.

The resulting mass matrices after EWSB are [20]

$$M_{\tilde{C}} = \begin{pmatrix} M_2 & \sqrt{2}s_{\beta}m_W \\ \sqrt{2}c_{\beta}m_W & \mu \end{pmatrix} \tag{A5}$$

in the $(\tilde{W}^+,\tilde{H}_u^+),(\tilde{W}^-,\tilde{H}_d^-)^T$ basis and

$$M_{\tilde{N}} = \begin{pmatrix} M_1 & 0 & -c_{\beta}s_W m_Z & s_{\beta}s_W m_Z \\ 0 & M_2 & c_{\beta}c_W m_Z & -s_{\beta}c_W m_Z \\ -c_{\beta}s_W m_Z & c_{\beta}c_W m_Z & 0 & -\mu \\ s_{\beta}s_W m_Z & -s_{\beta}c_W m_Z & -\mu & 0 \end{pmatrix}$$
(A6)

in the $(\tilde{B}, \tilde{W}^0, \tilde{H}_d^0, \tilde{H}_u^0)$ basis. These mass matrices are diagonalized by

$$M_{\tilde{C}} = U^T M_{\tilde{C}}^{(D)} V, \qquad M_{\tilde{N}} = N^T M_N^{(D)} N,$$
 (A7)

where U, V, and N are unitary matrices.

The electroweak sector of the MSSM, including the Higgs fields, generically violates CP symmetry with new physical phases. We will now count parameters and look at CP-violating invariants in this sector. This analysis has been done in ref. [22], but we reproduce it here with a different emphasis.

The electroweak sector has four complex parameters M_i , μ , b plus the real gauge couplings. We would like to determine how many of these parameters are physical. Note that the electroweak sector without potentials has a $U(1)_R \times U(1)_{PQ}$ global symmetry. The symmetry is explicitly broken by the superpotential and soft terms. There is no residual symmetry in the electroweak sector. We are thus able to remove two of the four complex phases in the parameters listed. There are two remaining physical phases in this sector.

Field	$U(1)_R$	$U(1)_{PQ}$
H_u	1	1
H_d	1	1

TABLE II. Charges of the (chiral) superfields under $U(1)_R \times U(1)_{PQ}$.

Spurion	$U(1)_R$	$U(1)_{PQ}$
M_i	-2	0
μ	0	-2
b	-2	-2

TABLE III. Charges of the spurions under $U(1)_R \times U(1)_{PQ}$.

Next, we would like to determine the invariants corresponding to these phases. For this, we perform a spurion analysis. The charges of the superfields under the symmetries are summarized in Table II. After writing these down, the charges of the spurions can be read off the potentials. The μ term conserves R charge, but violates PQ symmetry. In order to render that term invariant, μ would need to have a charge of -2. The gauginos are invariant under $U(1)_{PQ}$, but they break $U(1)_R$ since they are superpartners of the gauge bosons, which must have R charge 0. The gauginos have R charge 1, so the gaugino masses have a spurious R charge of -2. Finally, the b term violates both symmetries. $U(1)_{PQ}$ is violated as in the μ term, so b has the same R charge as μ . It also violates $U(1)_R$ since it should have R charge

0, not 2 as in the superpotential. b must then have a spurious R charge of 2. The charges of the spurions are summarized in Table III.

All observables must be proportional to Hermitian combinations of parameters that have 0 spurious charge. CP violating observables should be proportional to the imaginary part of combinations with 0 spurious charge. The imaginary part vanishes in the CP conserving case and renders the combination real. There are two classes of such observables in the current case. The first is the class of observables formed out of gaugino masses alone: $Im(M_1^*M_2)$. The other class of observables involves μ . Such observables must also involve b since it is the only other spurion with PQ charge. In particular, we must use the combination μ^*b , which has no PQ charge but has R charge -2. To form an invariant we must include one of the gaugino masses. However, the two possible such terms (one for each gaugino mass) are not independent since they can be written in terms of just one of the possible combinations, as well as combinations of only gaugino masses. In what follows, we will discuss only the electroweak sector. We will further neglect mixing with Bino for simplicity. This approximation is justified when the mass M_1 is much larger than M_2 , μ and b. Then, the only relevant CP violating invariant to study is

$$\operatorname{Im}(\mu^* b M_2^*). \tag{A8}$$

While there are generally strong bounds on this phase due to the non-observation of electric dipole moments [24], the bounds are model dependent. They come from loops involving the sleptons [25, 26]. We assume that we can make these loops small by, for example, making the sleptons very heavy, so that the region of parameter space we will study is not excluded by indirect measurements.

Appendix B: Differential Decay Rate of Heavy Neutralino

We use the notation of Ref. [27]. The differential decay rate of the heavy neutralino via the diagrams Fig. 6, $\chi_4^0 \to \chi_1^+ \chi_2^- \chi_1^0$, is given by

$$\frac{d\Gamma}{dq_{13}^2dq_{23}^2} = \frac{1}{(2\pi)^3} \frac{1}{32m_0^3} \\
= \frac{1}{(q_{13}^2 - m)^2 + \Gamma^2 m^2} \left[(m_0^2 + m_2^2 - q_{13}^2)(|\lambda_{02}^+|^2 + |\lambda_{02}^-|^2) + 4m_0 m_2 \operatorname{Re}(\lambda_{02}^+ \lambda_{02}^-) \right] \\
= \left[(q_{13}^2 - m_1^2 - m_3^2)(|\lambda_{31}^+|^2 + |\lambda_{31}^-|^2) - 4m_1 m_3 \operatorname{Re}(\lambda_{31}^+ \lambda_{31}^-) \right] + (1 \leftrightarrow 2) + \\
2\operatorname{Re} \left\{ \frac{1}{(q_{13}^2 - m^2 + im\Gamma)(q_{23}^2 - m^2 - im\Gamma)} \times \right. \\
\left. \left[m_0 m_1 (q_{23}^2 - m_2^2 - m_3^2)(\lambda_{32}^2 \lambda_{01}^{-*} \lambda_{02}^{-*} \lambda_{31}^{+*} + [+ \leftrightarrow -]^*) + \right. \\
\left. (q_{13}^2 q_{23}^2 - m_0^2 m_3^2 - m_1^2 m_2^2)(\lambda_{01}^+ \lambda_{32}^- \lambda_{02}^{-*} \lambda_{31}^{+*} + [+ \leftrightarrow -]^*) + \right. \\
\left. m_1 m_2 (q_{13}^2 + q_{23}^2 - m_1^2 - m_2^2)(\lambda_{02}^+ \lambda_{32}^- \lambda_{01}^{-*} \lambda_{31}^{+*} + [+ \leftrightarrow -]^*) + \right. \\
\left. m_0 m_3 (q_{13}^2 + q_{23}^2 - m_0^2 - m_3^2)(\lambda_{31}^- \lambda_{32}^- \lambda_{01}^{-*} \lambda_{31}^{-*} + [+ \leftrightarrow -]^*) + \right. \\
\left. m_0 m_2 (q_{13}^2 - m_1^2 - m_3^2)(\lambda_{01}^+ \lambda_{02}^+ \lambda_{32}^- \lambda_{31}^{-*} + [+ \leftrightarrow -]^*) + \right. \\
\left. m_1 m_3 (q_{13}^2 - m_0^2 - m_2^2)(\lambda_{01}^+ \lambda_{31}^- \lambda_{32}^- \lambda_{02}^{-*} + [+ \leftrightarrow -]^*) + \right. \\
\left. m_2 m_3 (q_{23}^2 - m_0^2 - m_1^2)(\lambda_{02}^+ \lambda_{31}^- \lambda_{32}^- \lambda_{01}^{-*} + [+ \leftrightarrow -]^*) - \right. \\
\left. 2m_0 m_1 m_2 m_3 (\lambda_{01}^+ \lambda_{02}^+ \lambda_{31}^- \lambda_{32}^- + [+ \leftrightarrow -]^*) \right] \right\} \right], \tag{B1}$$

where $m=m_{H^+}$, $\Gamma=\Gamma_{H^+}$, $m_0=m_{\chi_4^0}$, $m_1=m_{\chi_1^+}$, $m_2=m_{\chi_2^-}$, $m_3=m_{\chi_1^0}$, and $\lambda_{ij}^{\pm}=Y^{H^{\pm}\chi_{a(i)}^0\chi_j^{\mp}}$ with a(0)=4, a(3)=1, and j=1,2. The notation $[+\leftrightarrow-]^*$ means exchange $\lambda^{\pm}\leftrightarrow\lambda^{\mp*}$ with the same indices. The differential decay rate for $\chi_4^0\to\chi_1^-\chi_2^+\chi_1^0$ can be obtained from (B1) by interchanging the indices 1 and 2 at all places.

^[1] M. Kobayashi, T. Maskawa, Prog. Theor. Phys. 49, 652-657 (1973).

^[2] J. Charles et al. [CKMfitter Group Collaboration], Eur. Phys. J. C41, 1-131 (2005). [hep-ph/0406184].

^[3] M. Bona et al. [UTfit Collaboration], Phys. Rev. Lett. 97, 151803 (2006) [arXiv:hep-ph/0605213].

^[4] M. Bona et al. [UTfit Collaboration], JHEP 0803, 049 (2008). [arXiv:0707.0636 [hep-ph]].

^[5] M. Raidal, A. van der Schaaf, I. Bigi, M. L. Mangano, Y. K. Semertzidis, S. Abel, S. Albino, S. Antusch *et al.*, Eur. Phys. J. C57, 13-182 (2008). [arXiv:0801.1826 [hep-ph]].

- [6] G. Valencia, Phys. Rev. **D39**, 3339 (1989).
- [7] J. G. Korner, K. Schilcher, Y. L. Wu, Phys. Lett. **B242**, 119 (1990).
- [8] B. Kayser, Nucl. Phys. Proc. Suppl. 13, 487-490 (1990).
- [9] W. Bensalem, D. London, Phys. Rev. **D64**, 116003 (2001). [hep-ph/0005018].
- [10] A. Datta, D. London, Int. J. Mod. Phys. A19, 2505-2544 (2004). [hep-ph/0303159].
- [11] J. A. Aguilar-Saavedra, Phys. Lett. B **596**, 247 (2004) [arXiv:hep-ph/0403243].
- [12] G. Moortgat-Pick, K. Rolbiecki, J. Tattersall and P. Wienemann, JHEP 1001, 004 (2010) [arXiv:0908.2631 [hep-ph]].
- [13] A. Bartl, H. Fraas, S. Hesselbach, K. Hohenwarter-Sodek and G. A. Moortgat-Pick, JHEP 0408, 038 (2004) [arXiv:hep-ph/0406190].
- [14] P. Langacker, G. Paz, L. -T. Wang, I. Yavin, JHEP 0707, 055 (2007). [hep-ph/0702068 [HEP-PH]].
- [15] A. Pilaftsis, M. Nowakowski, Phys. Lett. **B245**, 185-191 (1990).
- [16] M. Nowakowski, A. Pilaftsis, Mod. Phys. Lett. A6, 1933-1942 (1991).
- [17] G. Eilam, J. L. Hewett, A. Soni, Phys. Rev. Lett. 67, 1979-1981 (1991).
- [18] D. Atwood, G. Eilam, M. Gronau, A. Soni, Phys. Lett. B341, 372-378 (1995). [hep-ph/9409229].
- [19] J. Berger, M. Blanke, Y. Grossman, work in progress.
- [20] S. P. Martin, arXiv:hep-ph/9709356.
- [21] H. E. Haber, Nucl. Phys. Proc. Suppl. **62**, 469 (1998) [arXiv:hep-ph/9709450].
- [22] S. Dimopoulos and S. D. Thomas, Nucl. Phys. B 465, 23 (1996) [arXiv:hep-ph/9510220].
- [23] I. Bediaga, I. I. Bigi, A. Gomes, G. Guerrer, J. Miranda and A. C. d. Reis, Phys. Rev. D 80, 096006 (2009) [arXiv:0905.4233 [hep-ph]].
- [24] K. Nakamura et al. [Particle Data Group Collaboration], J. Phys. G G37, 075021 (2010).
- [25] T. Ibrahim, P. Nath, Phys. Rev. D58, 111301 (1998). [hep-ph/9807501].
- [26] M. Brhlik, G. J. Good, G. L. Kane, Phys. Rev. **D59**, 115004 (1999). [hep-ph/9810457].
- [27] H. K. Dreiner, H. E. Haber, S. P. Martin, Phys. Rept. 494, 1-196 (2010). [arXiv:0812.1594 [hep-ph]].